

Microwave synthesis of metal doped TiO₂ for photocatalytic applications

J. Maragatha¹ · S. Rajendran² · T. Endo³ · S. Karuppuchamy¹

Received: 25 October 2016 / Accepted: 5 December 2016 / Published online: 30 December 2016
© Springer Science+Business Media New York 2016

Abstract Nanostructured metal (Sn, Cu and Ni) doped TiO₂ was successfully synthesized by microwave irradiation method. Metal doped TiO₂ was characterized by X-ray diffraction (XRD), Scanning electron microscope (SEM), Fourier transform infrared spectroscopy (FTIR) and UV–Vis spectroscopy (UV–Vis). The XRD pattern confirms the formation of monoclinic phase TiO₂ and metal doped TiO₂ samples. SEM images show the attractive morphologies for metal doped TiO₂ nanopowders. The photocatalytic activity of the synthesized sample was also studied by the decomposition of methylene blue dye under UV light irradiation.

1 Introduction

Photocatalytic effect at the surface of titanium dioxide has been attracting much interest to examine their useful applications for self cleaning of tiles, glasses, and windows, air and water purification [1]. Water pollution is one of the major contaminations in the world. Several treatments were used in order to solve this problem. Among them photocatalytic decomposition is one of the best method for waste water treatment. Since, the first discovery of photocatalytic splitting of water with TiO₂ under ultra violet (UV) light irradiation by Fujishima and Honda [2], the

semiconductor metal oxides (e.g., TiO₂, CdS, ZnS, Fe₂O₃ and ZnO) are attracting much attention for use in photocatalysis [3–16]. Titanium dioxide is one of the best semiconductor oxides due to its cost effective, eco-friendly nature, photostability, chemical inertness and high stability [17–23]. It has been potential material owing to its environmental applications such as photon-to-electric energy conversion devices or water-splitting applications and pollutant dissociation [24–26]. TiO₂ exists in three different crystalline polymorphic phases such as anatase, rutile and brookite [27]. The rutile and anatase phases have an energy band gap of 3.0–3.2 eV and hence it can absorb only <5% of the solar radiation that reaches the earth's surface [28]. For this function, doping or combining TiO₂ with different non-metal or transition metal ions has been initiated. In this work, Sn, Cu and Ni have been selected for doping with TiO₂. Tin is nontoxic, abundant, and inexpensive and has relatively high chemical stability. Sn-doped titania also illustrated improved day-light activity and it has a wide band gap of 3.8 eV [29, 30]. It is highly enviable to manipulate size distribution and design, surface chemistry and chemical composition of tin oxide nanocrystals reaction to visible-light, which accounts for 43% of the entire sunlight [31]. Cu is a relatively abundant and low cost metal [32] and it nearly inhibits electron–hole recombination to improve the catalyst. Some reports exposed that Cu-doped TiO₂ nanoparticles could be fabricated via a vapor-phase syntheses (e.g., evaporation condensation and sputtering) or liquid-phase syntheses (e.g., sol–gel and impregnation) [33]. Nickel has been established to be a capable transition metal for increasing the photocatalytic activity when it is doped with TiO₂. Ni-doped mesoporous TiO₂ catalyst played a major role in controlling the morphology and thermal stability of mesoporous photocatalysts [34, 35]. Transition metal doped titanium dioxides were synthesized by

✉ S. Karuppuchamy
skchamy@alagappauniversity.ac.in; skchamy@gmail.com

¹ Department of Energy Science, Alagappa University, Karaikudi, Tamil Nadu 630 003, India

² Department of Physics, Alagappa University, Karaikudi, Tamil Nadu 630 003, India

³ Molecular Engineering Institute, Kinki University, 11-6, Kayanomori, Iizuka, Fukuoka 820 8555, Japan

various methods such as sol–gel method [36], anodization method [37], electrospinning method [38], hydrothermal and solvothermal method [39], spin-coating technique [40] etc. These methods are tedious in contrast to the microwave irradiation method. The microwave irradiation method has sparked much attention owing to its simplicity, logically low cost, short period and likelihood of huge scale construction [41, 42]. In the present work, TiO_2 and metal doped TiO_2 nanomaterials were synthesized by microwave irradiation method and subsequently characterized the materials using several advanced techniques. The photocatalytic performance of the synthesized nano-sized TiO_2 and metal doped TiO_2 nanopowders was also investigated by methylene blue dye under the visible light irradiation.

2 Materials and methods

2.1 Materials

Commercially available titanium oxychloride (TiOCl_2), stannous chloride dihydrate, copper acetate monohydrate, nickel(II) acetate tetrahydrate, sodium hydroxide (NaOH), methylene blue, deionized water (DD) were used as received.

2.2 Experimental methods

Metal doped TiO_2 powders were prepared by microwave irradiation method using the following procedure. A mixture of 1.6 M titanium oxychloride (TiOCl_2) was prepared using deionized water as solvent and stirred at room temperature. Titanium precursor was added to the transition metals (0.1 M stannous chloride dihydrate, 0.1 M copper acetate monohydrate, 0.1 M nickel(II) acetate tetrahydrate) after stirring for 30 min. Sodium hydroxide (NaOH) solution was added dropwise until the pH of the solution reached 12 and maintained at 90 °C. After 1 h vigorous stirring, solution was obtained. Same procedure was followed and then added 1.6 M titanium oxychloride and NaOH without transition metals. The microwave irradiation was passed through the solution with the frequency of 2.45 GHz with power of 160 W for 30 min. Subsequently TiO_2 and metal doped TiO_2 powders were formed.

2.3 Photocatalytic measurement

The photocatalytic activities of the synthesized TiO_2 and metal doped TiO_2 nanomaterials were evaluated by the degradation of methylene blue under a 6-W UV lamp equipped with a cutoff filter ($\lambda > 254$ nm). The illumination intensity used for the photodegradation of dye was 6 W UV lamp—Philips. To keep the photocatalytic reaction at

room temperature, the reaction beaker was kept in a cooling water system. An amount of 0.1 g of photocatalyst was suspended in a 200 mL aqueous methylene blue (MB) dye solution (10 mg/L). Prior to the illumination, the suspensions were ultra-sonicated for 5 min under dark condition for 1 h to ensure an adsorption–desorption equilibrium of the MB dye was adsorbed to saturation level on the surface of catalysts. The effect of concentration of the catalysts on the degradation of dye was also investigated.

2.4 Characterization

The structural property of metal doped TiO_2 was studied by X-ray diffraction (XRD) using $\text{Cu-K}\alpha$ ($\lambda = 0.154$ nm) radiation source (X'pert Pro PANalytical) over a 2θ scan range of 10–80°. Morphological studies of the samples were examined by Scanning Electron Microscope (SEM; JEOL JCM-6000, 15 KV). The quality and composition of the nanoparticles were characterized by Perkin Elmer-Fourier transform infrared (FT-IR) spectrometer in the range of 400–4000 cm^{-1} in KBr pellets. The MB dye degradation was measured by UV–Vis spectrophotometer (SCHIMADZU UV-1800) in the wavelength range of 400–800 nm.

3 Results and discussion

3.1 X-ray diffraction (XRD)

The as-prepared TiO_2 and metal (Sn, Cu and Ni) doped TiO_2 powder was found to be crystalline nature. The XRD pattern was also measured for the samples which were subjected to microwave irradiation for 30 min. Figure 1a–d shows the XRD pattern of the synthesized TiO_2 and metal (Sn, Cu and Ni) doped TiO_2 powders. XRD pattern of TiO_2 powder is well indexed to the standard pattern of monoclinic phase which is in accordance with the JCPDS card no.481278. The sharper peaks clearly indicate the presence of TiO_2 . The pure TiO_2 peak was large compared to those of metal doped TiO_2 samples. The X-ray powder diffraction patterns were also used to determine the crystallite size of all the prepared samples. The crystallite size D was determined from the broadening of the peaks by Scherrer's formula.

$$D = K\lambda/\beta \cos \theta$$

where K is the shape factor (0.9), λ is the wavelength, β is the width of the peak at half the maximum intensity (FWHM) after subtraction of instrumental noise, and θ is the diffraction angle. The estimation shows that the mean crystallite size of TiO_2 and metal (Sn, Cu and Ni) doped

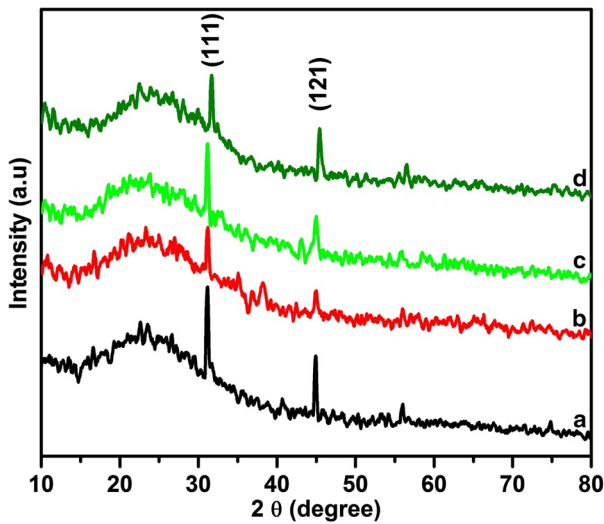


Fig. 1 XRD pattern of *a* pure TiO₂, *b* Sn doped TiO₂, *c* Cu doped TiO₂ and *d* Ni doped TiO₂ for microwave irradiation for 30 min

TiO₂ are in the range of 57 nm and 20 nm, 27 nm and 30 nm respectively.

3.2 SEM with EDX analysis

SEM images of TiO₂ and metal (Sn, Cu and Ni) doped TiO₂ powders are shown in Fig. 2. The SEM image of TiO₂ and metal (Sn, Cu and Ni) doped TiO₂ powder indicates the presence of particles of different shapes and sizes. Figure 2a display the SEM image of pure TiO₂ sample and it clearly indicates the aggregation of particles. The addition of various doping materials such as Sn, Cu and Ni influences the surface morphology of the TiO₂ powder. Figure 2b shows the SEM image of Sn-TiO₂ powder and it clearly evinces the formation of nanoparticle. Figure 2c shows the image of Cu-TiO₂ sample and it clearly point out the formation of flower like structure. Careful observation of SEM image of Ni-TiO₂ sample shows the presence of nanoplate morphology (Fig. 2d). Figure 3a–c show the EDX spectra of TiO₂, Sn doped TiO₂ and Ni doped TiO₂

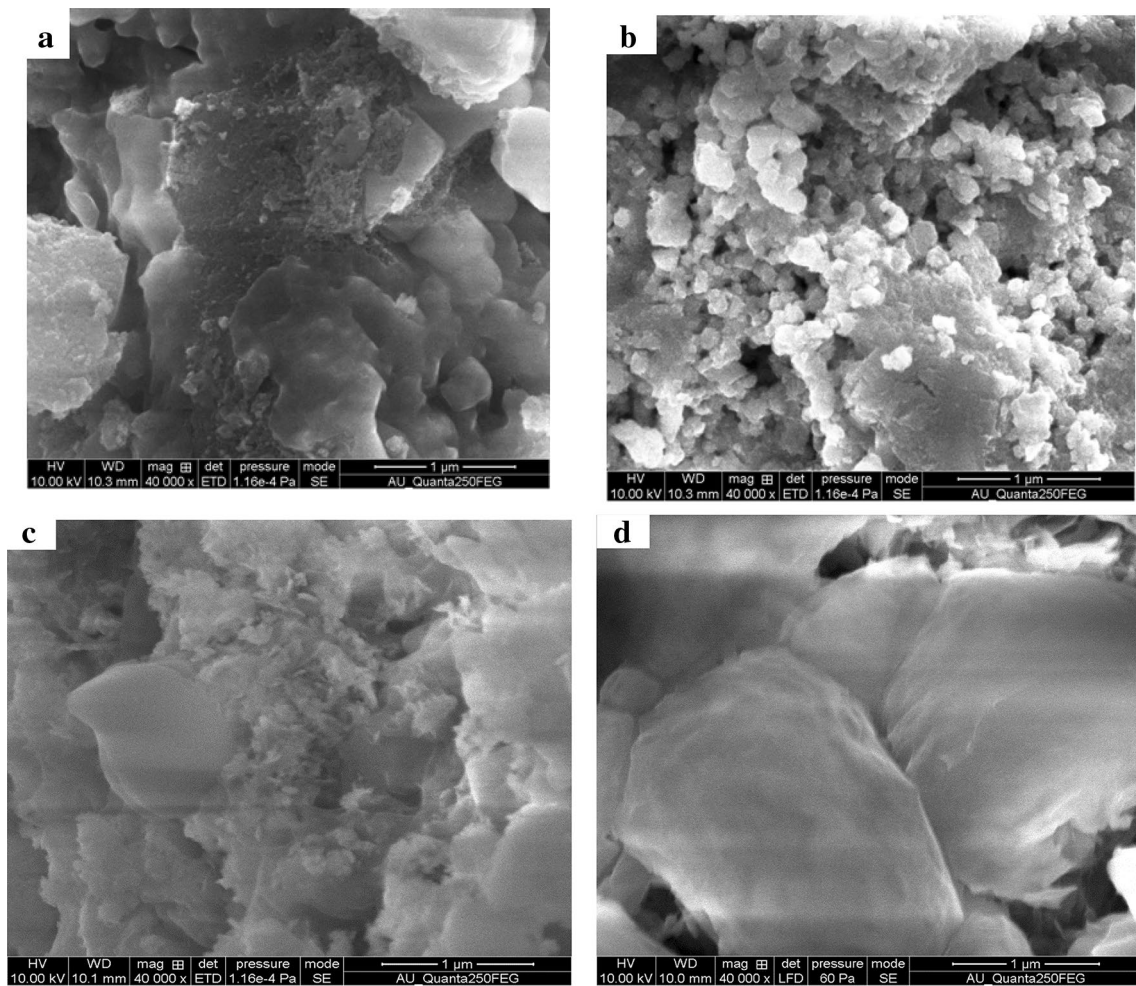


Fig. 2 SEM image of *a* pure TiO₂, *b* Sn doped TiO₂, *c* Cu doped TiO₂ and *d* Ni doped TiO₂ for microwave irradiation for 30 min

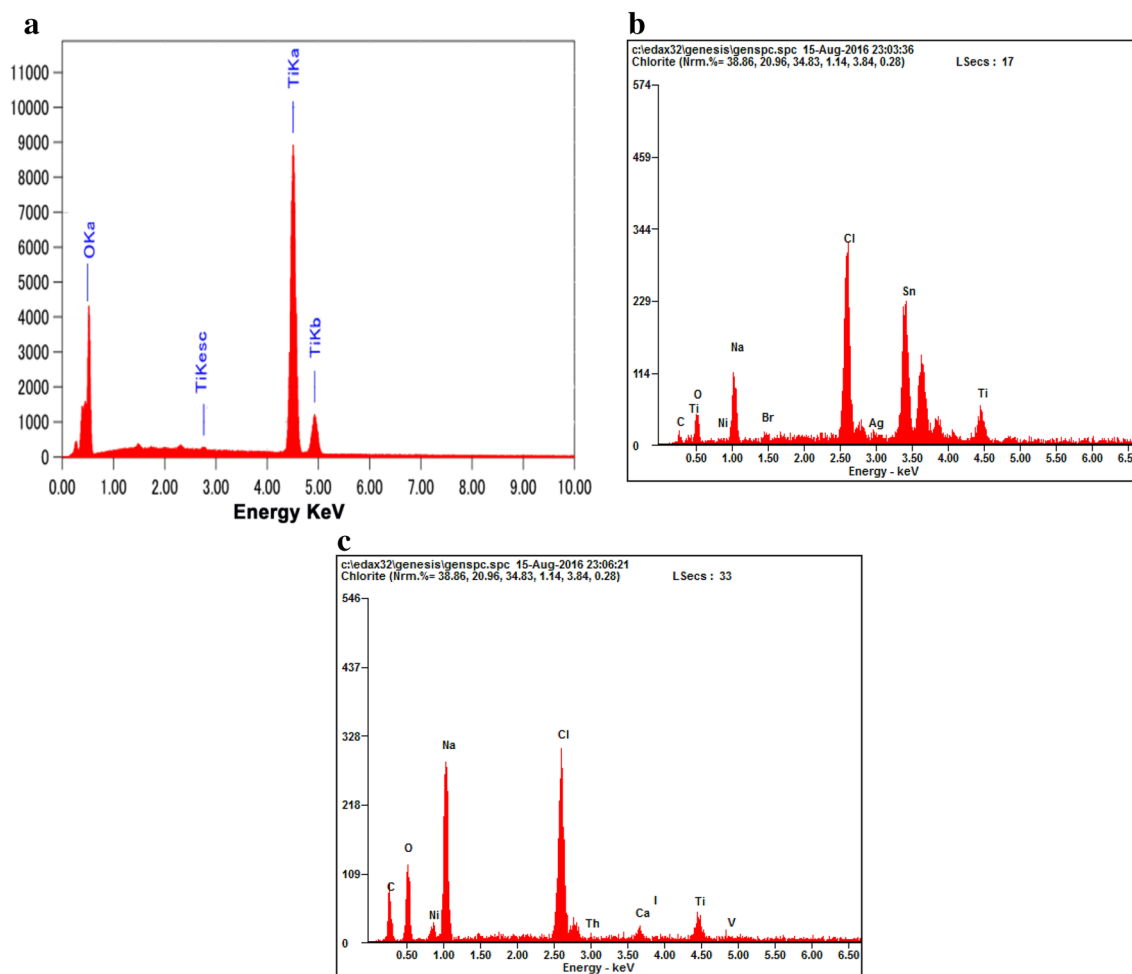


Fig. 3 EDX spectra of **a** pure TiO_2 , **b** Sn doped TiO_2 and **c** Ni doped TiO_2 for microwave irradiation for 30 min

and the EDX spectra confirms the presence of Ti, Sn, O and Ni elements, respectively.

3.3 Fourier transform infrared spectroscopy (FTIR)

Figure 4 shows FTIR spectra of TiO_2 and metal (Sn, Cu and Ni) doped TiO_2 samples in the range of $400\text{--}4000\text{ cm}^{-1}$ at room temperature. The bands observed in the range of $400\text{--}800\text{ cm}^{-1}$ are mainly ascribed to Ti–O and Ti–O–O bonds. Since Ti–O bond is shorter than Sn–O, Cu–O and Ni–O bonds therefore, the doping of metal in TiO_2 may lead to a shift of the wavenumber of Ti–O lattice vibration [43–45]. The bands observed in the range of 1101 and 1026 cm^{-1} are present in all the samples which indicate Ti–O–Ti vibrations [34]. The band at 1445 cm^{-1} in TiO_2 has been attributed to stretching vibration of Ti–O–Ti group which is shifted to 1409 cm^{-1} . This may be due to the doping metals in of TiO_2 [46]. The stretching vibration of O–H and bending vibration of the adsorbed water molecules are also present at 1645 cm^{-1} in TiO_2 and Sn doped TiO_2 . Then

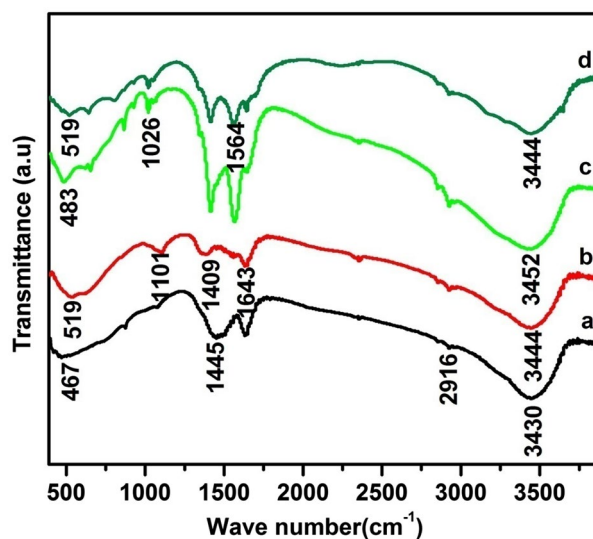


Fig. 4 FTIR spectra of **a** pure TiO_2 , **b** Sn doped TiO_2 , **c** Cu doped TiO_2 and **d** Ni doped TiO_2 for microwave irradiation for 30 min

Cu and Ni doped into TiO_2 the peak shifted to 1564 cm^{-1} this may be due to the doping of Cu and Ni [34]. The peaks observed at 2922 cm^{-1} corresponds to residue of bioorganic substances [47]. The presence of an intense H_2O band at $3430, 3444$ and 3452 cm^{-1} confirms the presence of hydroxyl groups or adsorbed water [30].

3.4 Ultraviolet visible spectroscopy (UV–Vis)

Figure 5a–d shows UV–Vis spectra of methylene blue dye in the presence of TiO_2 and metal (Sn, Cu and Ni) doped TiO_2 sample under UV light. Microwave treatment for 30 min under the irradiation of light above 254 nm was performed for the sample. The peak intensity of methylene blue dye absorption was found at 665 nm and the intensity of the methylene blue absorption decreased with an increase of the reaction time from 0 to 3 h [48].

$$\eta\% = (\text{abs}_0 - \text{abs}_t) \times 100/\text{abs}_0$$

3.5 Photocatalytic activity test

Photocatalytic activity of the synthesized TiO_2 and metal (Sn, Cu and Ni) doped TiO_2 samples was performed by the degradation of Methylene Blue (MB) in aqueous solution under UV light irradiation. MB shows a maximum absorption at about 665 nm. Figure 6a–d shows the decomposition of MB in aqueous solution in the presence of TiO_2 and metal (Sn, Cu and Ni) doped TiO_2 which was prepared by the microwave treatment. The MB degradation study was carried out under UV light irradiation ($\lambda > 254\text{ nm}$). The degradation efficiency of the samples was defined as C/C_0 , where C and C_0 stood for the remnants and initial concentration of MB. The degradation efficiency of MB was calculated as 92, 85, 60 and 54% for the samples TiO_2 , Sn– TiO_2 , Cu– TiO_2 and Ni– TiO_2 , respectively. The activity of the TiO_2 photocatalytic efficiency was high compared to metal doped TiO_2 . This is due to the change of number of active sites, surface group type (or) acid-base properties in the metal (Sn, Cu and Ni) doped TiO_2 samples which depends on the ionic radius, charge and low diffusion

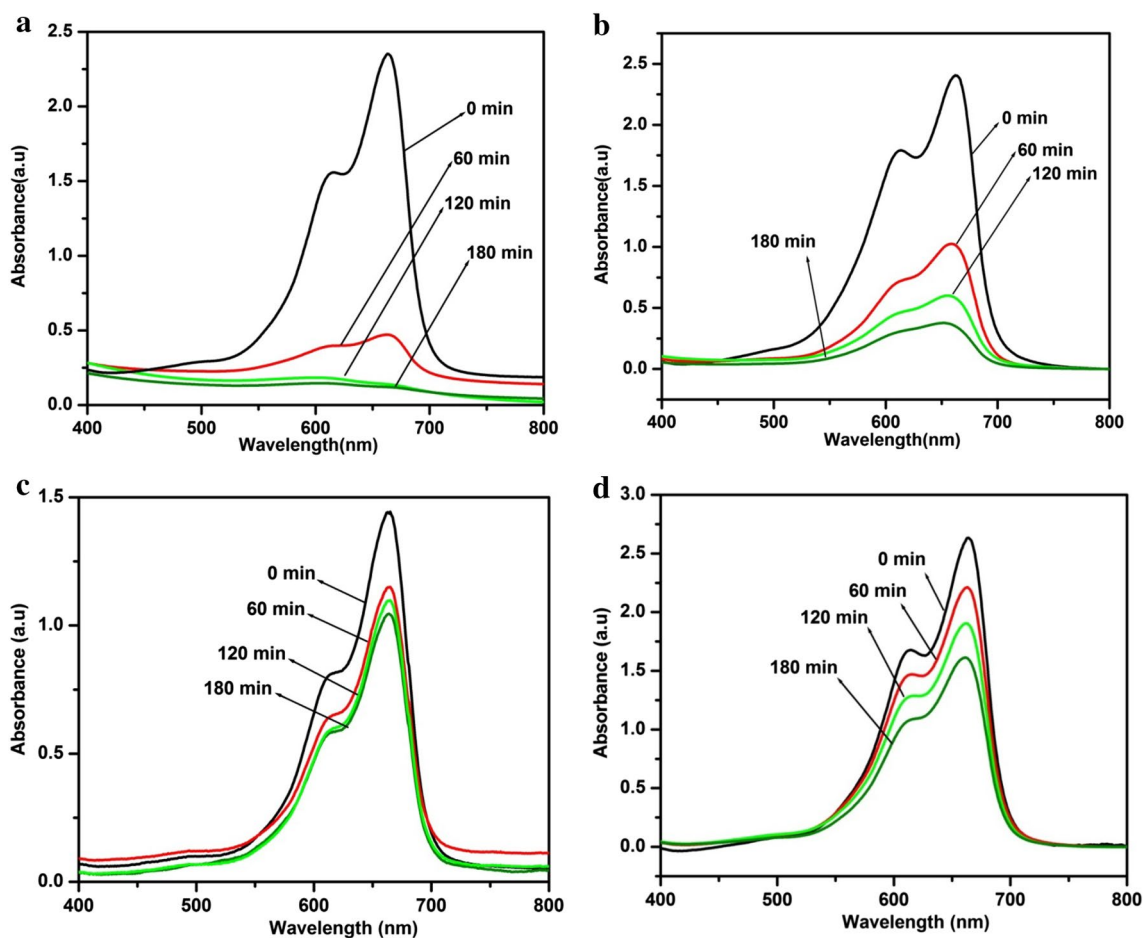


Fig. 5 UV–Vis Spectra of **a** pure TiO_2 , **b** Sn doped TiO_2 , **c** Cu doped TiO_2 and **d** Ni doped TiO_2 for microwave irradiation for 30 min

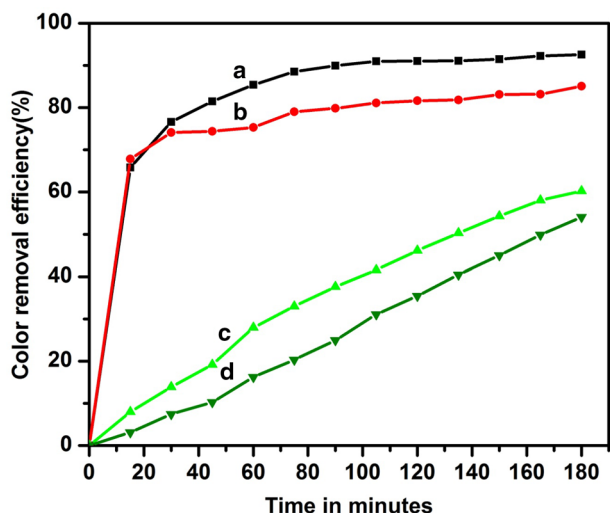


Fig. 6 Photocatalytic degradation of MB in presence of *a* pure TiO₂, *b* Sn doped TiO₂, *c* Cu doped TiO₂ and *d* Ni doped TiO₂ for microwave irradiation for 30 min. Reaction conditions: (MB)=10 ppm, V=200 mL, (Catalyst)=0.1 gL⁻¹, Light intensity = 6 W

length. This also serves as a trap for the electron produced under irradiation [49].

4 Conclusions

The pure TiO₂ and metal (Sn, Cu and Ni) doped TiO₂ photocatalyst was successfully synthesized by microwave irradiation method. The XRD pattern confirmed the formation of monoclinic TiO₂ and metal (Sn, Cu and Ni) doped TiO₂. SEM image revealed the morphology of the prepared samples. FTIR studies confirmed the functional groups. The prepared pure TiO₂ and metal (Sn, Cu and Ni) doped TiO₂ photocatalyst successfully decomposed the methylene blue dye under UV light irradiation.

Acknowledgements The authors are grateful to the Department of physics and chemistry, Alagappa University for providing the XRD, SEM and FTIR characterization facilities.

References

1. A. Zaleska, *Recent Pat. Eng.* **2**, 157–164 (2008)
2. Z. Zhang, Y. Zhou, Y. Zhang, X. Sheng, S. Zhou, S. Xiang, *Appl. Surf. Sci.* **286**, 344–350 (2013)
3. B. Pant, H.R. Pant, N.A.M. Barakat, M. Park, K. Jeon, Y. Choi, H.Y. Kim, *Ceram. Int.* **39**, 7029–7035 (2013)
4. S. Karuppuchamy, M. Iwasaki, H. Minoura, *Vacuum* **81**, 708–712 (2007)
5. T. Furukawa, H. Matsui, H. Hasegawa, S. Karuppuchamy, M. Yoshihara, *Solid State Commun.* **142**, 99–103 (2007)

6. S. Yamamoto, H. Matsui, S. Ishiyama, S. Karuppuchamy, M. Yoshihara, *Mater. Sci. Eng. B* **135**, 120–124 (2006)
7. H. Matsui, T. Kawahara, R. Kudo, M. Uda, S. Karuppuchamy, M. Yoshihara, *J. Alloys Compd.* **462**, 20–23 (2008)
8. H. Matsui, S. Karuppuchamy, J. Yamaguchi, M. Yoshihara, *J. Photochem. Photobiol. A Chem.* **189**, 280–285 (2007)
9. H. Matsui, T. Kuroda, K. Otsuki, K. Yokoyama, T. Kawahara, S. Karuppuchamy, M. Yoshihara, *Tanso* **222**, 114–117 (2006)
10. M. Thamima, S. Karuppuchamy, *Adv. Sci. Eng. Med.* **7**, 18–25 (2015)
11. T. Oekermann, S. Karuppuchamy, T. Yoshida, D. Schlettwein, D. Wohlr, H. Minoura, *J. Electrochem. Soc.* **151**, 62–68 (2004)
12. S. Karuppuchamy, S. Ito, *Vacuum* **82**, 547–550 (2008)
13. H. Miyazaki, H. Matsui, T. Kuwamoto, S. Ito, S. Karuppuchamy, M. Yoshihara, *Micropor. Mesopor. Mater.* **118**, 518–522 (2009)
14. H. Miyazaki, H. Matsui, Y. Kita, S. Karuppuchamy, S. Ito, M. Yoshihara, *Curr. Appl. Phys.* **9**, 155–160 (2009)
15. R. Dhilip Kumar, S. Karuppuchamy, *J. Mater. Sci. Mater. Electron.* **26**, 3256–3261 (2015)
16. H. Matsui, N. Bandou, S. Karuppuchamy, M.A. Hassan, M. Yoshihara, *Ceram. Int.* **38**, 1605–1610 (2012)
17. A.M.H. Milad, L.J. Minggu, M.B. Kassim, W.R.W. Daud, *Ceram. Int.* **39**, 3731–3739 (2013)
18. S. Karuppuchamy, N. Suzuki, S. Ito, T. Endo, *Curr. Appl. Phys.* **9**, 243–248 (2009)
19. K. Santhi, P. Manikandan, C. Rani, S. Karuppuchamy, *Appl. Nanosci.* **5**, 373–378 (2015)
20. N. Suzuki, S. Karuppuchamy, S. Ito, *J. Appl. Electrochem.* **39**, 141–146 (2009)
21. H. Matsui, T. Okajima, S. Karuppuchamy, M. Yoshihara, *J. Alloy. Compd.* **468**, 27–32 (2009)
22. H. Matsui, S. Nagano, S. Karuppuchamy, M. Yoshihara, *Curr. Appl. Phys.* **9**, 561–566 (2009)
23. H. Matsui, Y. Saitou, S. Karuppuchamy, M.A. Hassan, M. Yoshihara, *J. Alloy. Compd.* **538**, 177–182 (2012)
24. S. Lee, Y. Lee, D.H. Kim, J.H. Moon, *Appl. Mater. Interfaces* **5**, 12526–12532 (2013)
25. S. Karuppuchamy, Y. Andou, T. Endo, *Appl. Nanosci.* **3**, 291–293 (2013)
26. N. Okada, S. Karuppuchamy, M. Kurihara, *Chem. Lett.* **34**, 16–17 (2005)
27. K. Palanivelu, J.S. Im, Y.S. Lee, *Carbon Sci.* **8**, 214–224 (2007)
28. W.I. Nawawi, M.A. Nawi, *J. Mol. Catal. A Chem.* **374–375**, 39–45 (2013)
29. H. Sayilkan, *Appl. Catal. A General* **319**, 230–236 (2007)
30. V.B.R. Boppana, R.F. Lobo, *ACS Catal.* **1**, 923–928 (2011)
31. C.M. Fan, Y. Peng, Q. Zhu, L. Lin, R.X. Wang, A.W. Xu, *J. Phys. Chem. C* **1172**, 24157–24166 (2013)
32. T.D. Pham, B.K. Lee, *Appl. Surf. Sci.* **296**, 15–23 (2014)
33. C.Y. Tsai, H.C. Hsi, T.H. Kuo, Y.M. Chang, J.H. Liou, *Aerosol. Air Qual. Res.* **13**, 639–648 (2013)
34. A.K. Tripathi, M.C. Mathpal, P. Kumar, V. Agrahari, M.K. Singh, S.K. Mishra, M.M. Ahmad, *Adv. A. Agarwal. Mater. Lett.* **6**, 201–208 (2015)
35. K.J. Salem, M.T. Hammad, R.R. Harrison, *J. Mater. Sci. Mater. Electron.*, **24**, 1670–1676 (2013)
36. S. Cizauskaitė, V. Reichlova, G. Nenartaviciene, A. Beganskiene, J. Pinkas, A. Kareiva, *Mater. Sci.* **25**, 3 (2007)
37. B. Samran, P. Krongkitsiri, S. Pimmongkol, S. Budngam, U. Tipparach, *Adv. Mater. Res.* **802**, 104–108 (2013)
38. J. Vonch, A. Yarin, C.M. Megaridis, *J. Undergraduate Res* **1**, 1 (2007)
39. S. Komarneni, *Curr. Sci.* **85**, 12 (2003)
40. Y.Y. Huang, K.S. Chou, *Ceram. Int.* **29**, 485–493 (2003)
41. R. Dhilip Kumar, S. Karuppuchamy, *J. Mater. Sci. Mater. Electron.* **26**, 6439–6443 (2015)

42. R. Dhillip Kumar, S. Karuppuchamy, *Ceram. Int.* **40**, 12397–12402 (2014)
43. M.R. Mahmoudian, W.J. Basirun, Y. Alias, M. Ebadi, *Appl. Surf. Sci.* **257**, 8317–8325 (2011)
44. N. Wongpisutpaisan, N. Vittayakorn, A. Ruangphanit, W. Pecharapa, *Sains Malaysiana* **42**, 175–181 (2013)
45. G. Viruthagiri, P. Praveen, S. Mugundan, E. Gopinathan, *Indian J. Adv. Chem. Sci.* **1**, 132–138 (2013)
46. E.H. Faria, A.L. Marçal, E.J. Nassar, K.J. Ciuffi, P.S. Calefi, *Mater. Res.* **10**, 413–417 (2007)
47. P. Dhandapani, S. Maruthamuthu, G. Rajagopal, J. Photochem. Photobiol. B Biol. **110**, 43–49 (2012)
48. J. Maragatha, K. Jothivenkatachalam, S. Karuppuchamy, *J. Mater. Sci. Mater. Electron.* **27**, 9233–9239 (2016)
49. S.N.R. Inturi, T. Boningari, M. Suidan, P.G. Smirniotis, *Appl. Cata. B Environ.* **144**, 333–342 (2014)